Analysis of Meis2 knockout mice reveals Sonic hedgehog-mediated patterning of the cochlear duct

[1,2]Hei Yeun Koo, [1,2]Jae Hwan Oh, [3]María Beatriz Durán Alonso, [3]Iris López Hernández, [3]Margarita González-Vallinas, [3]María Teresa Alonso, [4]Juan J Tena, [4]Alejandro Gil-Gálvez, [5]Fernando Giraldez, [1,2]Jinwoong Bok and [3]Thomas Schimmang*

[1]Department of Anatomy, Yonsei University College of Medicine, Seoul 03722, Korea

[2]Brain Korea 21 Project for Medical Science, Yonsei University College of Medicine, Seoul 03722, Korea

[3]Unidad de Excelencia, Instituto de Biomedicina y Genética Molecular de Valladolid (IBGM), Universidad de Valladolid y Consejo Superior de Investigaciones Científicas (CSIC), c/ Sanz y Forés 3, Valladolid 47003, Spain

[4]Centro Andaluz de Biología del Desarrollo (CABD), Consejo Superior de Investigaciones Científicas (CSIC)/Universidad Pablo de Olavide, 41013 Sevilla, Spain

[5]Dept. Medicine and Life Sciences (MELIS) CEXS, Universitat Pompeu Fabra, María de Maeztu Unit of Excellence, Parc de Recerca Biomédica de Barcelona (PRBB), Barcelona, Spain

*Corresponding author

Abstract

Background: The mechanisms underlying the formation of complex structures such as during the outgrowth of the cochlear duct are still poorly understood.

Results: We have analyzed the morphological and molecular changes associated with cochlear development in mouse mutants for the transcription factor Meis2, which show defective coiling of the cochlea. These morphological abnormalities were accompanied by the formation of ectopic and extra rows of sensory hair cells. Gene profiling of otic vesicles from Meis2 mutants revealed a dysregulation of genes that are potentially involved in Sonic hedgehog (Shh)-mediated patterning of the cochlear duct. Like in Shh mutants, Meis2 defective mice showed a loss of genes that are expressed in the apical part of the cochlear duct.

Conclusions: Taken together, these data reveal that the loss of Meis2 leads to a phenotype that resembles Shh mutants, suggesting that Meis2 is instrumental for cochlear Shh signaling. The modulation of the same subset of genes provides an interesting insight into which Shh responsive genes are essential for outgrowth and patterning of the cochlear duct.

Introduction

In mammals, the development of the inner ear is a prime example for the complexity underlying organ formation. It contains domains with a most unique organization such as the semicircular canals or the cochlea. They contain the sensory organs for hearing and balance which comprise hair cells that sense sound, gravity and acceleration. Within the cochlea, hair cells are the sensory transducers, which are arranged in a complex and precise mosaic pattern in rows that requires the coordinated expression of specific genes[1,2].

The cochlea is a spiral organ which is organized tonotopically. i.e.: hair cells tuned to different sound wave frequencies are located in different locations along the axis of the cochlea. During mammalian development, the cochlear duct undergoes a process of elongation, bending and coiling to form a spiral. These morphogenetic processes are regulated by signaling pathways such as those controlled by Wnt, components of the planar cell polarity (PCP) pathway or Sonic hedgehog (Shh), which has been shown to control elongation and regional specification of the cochlear duct[1]. Before mouse embryonic day 11 (E11), Shh is expressed in the floor plate and notochord from where it specifies ventral and regional identity in the otic vesicle and cochlea, respectively[3-5]. Thereafter, Shh is found in the cochlear ganglion from where it regulates cochlear extension and differentiation[5,6]. A comprehensive list of Shh-responsive genes expressed during initiation of cochlear duct formation has been reported recently, which provides a useful reference for deciphering Shh-dependent regulatory mechanisms[7].

Transcription factors act as key regulators during the development of the cochlear duct[8-15], however, their downstream networks are often poorly understood. In the case of Meis transcription factors, retinoic acid, Wnts and Fgfs have been proposed to be instrumental signaling components[16]. In this study we have explored the signaling pathways downstream of Meis2 in the mammalian otic vesicle by using RNAseq analysis of Meis2 mutants. We reveal that a subset of Shh-regulated genes are dysregulated in these mutants which phenotypically resemble mutants with a partial loss of Shh signaling. This indicates that Meis-mediated Shh signaling is required for proper cochlear development.

Results

We had recently observed that mouse mutants lacking Meis2 in the otic vesicle showed either a complete absence of (*Meis2*$^{flox/flox}$; *Foxg1*$^{Cre/+}$) or an abnormal (*Meis2*$^{flox/flox}$; *Pax2*$^{Cre/+}$) cochlear outgrowth during inner ear development[17,18]. To further define the phenotype associated with *Meis2*$^{flox/flox}$; *Pax2*$^{Cre/+}$ mutants, cochleae were dissected at E18.5 and stained with phalloidin and myosin VIIA antibodies to label hair cells. In *Meis2*$^{flox/flox}$; *Pax2*$^{Cre/+}$ cochleae, cochlear length was severely shortened as compared to wild type (Fig. 1A,E). In addition, mutant samples showed four or five rows of outer hair cells instead of the normal three rows (compare Figs. 1B-D´, control, and Fig. 1. F-H´, mutant). Similar phenotypes have been previously observed in other mouse mutants lacking transcription factors like *Neurog1, Neurod1, N-myc* and *Foxg1*[10,12,19,20]. In addition,

ectopic vestibular-like hair cells were observed in the greater epithelial ridge (GER) region of the apical cochlea (Fig. 1. I-J´´).

The first phenotypic change observed in *Meis2*$^{flox/flox}$; *Pax2*$^{Cre/+}$ mutants was the reduced size of the otic vesicle[17]. During normal development, cochlear morphogenesis is initiated at the ventral portion of the otic vesicle by an elongation that later on coils in an anterior–medial direction until it completes one and three−quarters turns (Fig. 1A and 3E). In contrast, in *Meis2*$^{flox/flox}$; *Pax2*$^{Cre/+}$ mutants the cochlear duct initially extends toward the apex but then takes a U-turn toward the base leading to a truncated cochlear duct[17] (Fig. 1E and 3J,O). In order to identify target genes of Meis2 with a potential developmental value for this process, we performed a RNAseq-based screen for differential gene expression in *Meis2*$^{flox/flox}$; *Pax2*$^{Cre/+}$ mutant versus wild-type otic vesicles at E11,5, the stage at which the outgrowth of the cochlear duct is initiated. The results of this analysis showed only 14 genes dysregulated in mutant samples, the majority of them being expressed during inner ear development (Table 1).

Most interestingly, we found that more than half of the differentially expressed transcripts in *Meis2*$^{flox/flox}$; *Pax2*$^{Cre/+}$ mutant otic vesicles (57%) showed a pattern of gene dysregulation which faithfully matched that of Shh mutant otic vesicles, genes that were either up- or down-regulated in parallel[7] (Table 1 and Figure 2A). This is a rather high figure when compared to other mouse mutants that show defects in cochlear outgrowth and from which transcriptomic data are available at the otic vesicle stage. Dysregulation of Shh-responsive genes is of 8% of the differentially expressed transcripts in *Chd7/Sox2* double mutants[21], 9% in *Tbx2/3* double mutants[14], 10% in *Six1* mutants[22], 11% in *Chd7* mutants[23] and 12% in

mutants expressing a dominant negative Fgf receptor[24] (see supplementary Table S1 for gene lists). Shh-responsive genes that were down-regulated in *Meis2*$^{flox/flox}$; *Pax2*$^{Cre/+}$ mutant otic vesicles included *cytochrome P450 family 26 subfamily C member 1* (*Cyp26c1), Follistatin (Fst), Fras1 related extracellular matrix protein 2 (Frem2), clusterin (Clu)* and *basal cell adhesion molecule (Bcam)*. Upregulated genes were *activated leukocyte cell adhesion molecule (Alcam)*, *calcium voltage-gated channel subunit alpha1 G (Cacna1g)* and *collagen type XII alpha 1 chain* (*Col12a1*). Differential regulation of *Cyp26c1, Fst, Frem2* and *Clu* was validated by RT-qPCR (Supplementary Figure 1).

In order to obtain insight into the transcriptional mechanisms regulating Meis2 target gene expression in the inner ear, we analyzed Transposase-Accessible Chromatin with high throughput sequencing (ATAC-Seq) data from chromatin isolated from wild-type otic vesicles[25,26]. ATAC-seq profiles from otic vesicles revealed more than 16,000 regions of open chromatin accessibility that mapped to intergenic (31%), intronic (30%), promoter (30%) and exonic (3%) regions of the genome (Fig. 2B). Gene regulatory sequences typically reside within regions of open chromatin[15,27,28]. In agreement, actively transcribed genes in the otic vesicle (RNA-seq, RPKM≥5) were more likely to display ATAC-seq signals than inactive genes (RNA-seq, RPKM<5) (Fig. 2C).

A comparison of Meis2-regulated genes and ATAC-seq analysis of otic vesicles showed that with the exception of *Acta2,* all genomic regions of the dysregulated genes contained accessible chromatin (Table 1). In order to identify potential Meis-dependent regulatory sequences associated with the differentially regulated Shh-responsive genes, we performed a search for Meis consensus binding sites[16] in genes exhibiting open chromatin regions as

revealed by ATAC-seq analysis. This analysis showed the presence of motifs for direct binding of the Meis transcription factor in the Shh-regulated genes *Cyp26c1, Frem2, Alcam* and *Bcam* (Table 1 and Figure 2A). The absence of Meis binding sites in other differentially regulated Shh-responsive genes suggests that they are indirectly regulated by Meis2.

Like Meis2 mutants, Shh defective mice are frequently characterized by a shortened cochlear duct, multiple rows of hair cells in the apex and ectopic vestibular-like hair cells[6,29,30]. Specification of regional identity along the cochlear duct depends on a gradient of Shh that leads to differences in hair cell morphology and physiology and the tonotopic organization of the cochlea: hair cells at the basal cochlea tune to high frequency sounds and those at the apex tune to low frequencies[2,5,10]. We thus asked whether loss of Meis2 also leads to changes in regional cochlear identity. To do so we analyzed expression patterns of genes, which are expressed in either a basal-to-apical or apical-to-basal gradient along the developing cochlea. E14.5 wild-type controls showed a distinct *A2m* and *Inhba* expression in the base of the cochlea (Fig. 3C,D), while *Msx1* and *Fst* were expressed in the apical end (Fig.3A,B). In *Meis2*$^{flox/flox}$; *Pax2*$^{Cre/+}$ cochleae, the basal markers were maintained in the basal turn (*A2m, Inhba*) (Fig.3H,I), but the apical markers were either lost (*Msx1* in Fig. 3K, asterisk) or weakly expressed (*Fst* in Fig.3L, arrow). These expression gradients revealed that *Meis2*$^{flox/flox}$*; Pax2*$^{Cre/+}$ mutants displayed an apically truncated cochleae, very much like the Shh deficit, which suggested a potential damage in the Shh signaling pathway in Meis2 mutants[5,29]. To further reveal if Shh signaling was affected in *Meis2*$^{flox/flox}$*; Pax2*$^{Cre/+}$ mutants, we examined the expression of the direct Shh target genes *Ptch1* and *Gli1*. In wild-type controls, *Ptch1* and *Gli1* are expressed in a graded pattern, stronger in the apex and

gradually weaker toward the base (Supplementary Fig.2A,B). In agreement with an alteration of cochlear Shh signaling, *Meis2*$^{flox/flox}$; *Pax2*$^{Cre/+}$ mutant showed strongly reduced expression of *Ptch1* and *Gli1* in the shortened cochlea (Supplementary Fig.2C,D).

Within the developing cochlea, regional identity is sequentially defined via Shh from two different sources: first, from the floor plate and the notochord in the ventral midline and, later on, starting at E11.75 from the spiral ganglion neurons[5,6]. A complete loss of Shh signaling leads to absence of all cochlear structures and the otic vesicles show a dysregulation of several markers such as *Pax2*, *Ngn1* and *Tbx1* which are, however, maintained in *Meis2*$^{flox/flox}$; *Pax2*^{Cre} mutants[3,4,17]. Therefore, *Meis2*$^{flox/flox}$; *Pax2*^{Cre} mutants are phenotypically close to mouse mutants with a partial rather than a complete loss of Shh signaling, including a truncated cochlea and ectopic rows of hair cells[6,30]. In *Shh*$^{flox/-}$; *Foxg1*^{Cre} mutants, in which Shh signaling from the spiral ganglion but not the ventral midline is selectively abolished, the cochlea is severely shortened, reaching only a half turn, very much like our to *Meis2*$^{flox/flox}$; *Pax2*^{Cre} mutant[6,17]. However, unlike in *Shh*$^{flox/-}$; *Foxg1*^{Cre} mutant mice[5], the expression domains of apical genes like *Fst* and *Msx1* are more affected in *Meis2*$^{flox/flox}$; *Pax2*^{Cre} mutants, indicating a potential crucial requirement of Meis2 for apical identity and cochlear outgrowth (Table 2).

To our knowledge, there is no co-expression of *Meis2* and Shh-target genes, the former found in the dorsal portion of the otic vesicle[17] and the latter mostly detected in its ventral portion[7]. However, at earlier stages of otic development, *Fst* and *Meis2* are both expressed in the otic placode[17,32]. Additionally, *Fst*, and the Shh target genes *Frem2, Cacna1g and*

Bcam show a relatively high expression in microarrays hybridized with RNA extracted from the otic placode [33].

Amongst the group of Meis2–regulated Shh responsive genes, *Cyp26c1, Clu* and *Fst* are expressed in the ventral portion of the otic vesicle (Table 1) from which the cochlear duct is derived. Loss of *Cyp26c1* does not affect embryonic development, but is required redundantly with *Cyp26a1* to regulate anterior–posterior patterning of the developing brain and the size of the otic vesicle[34]. *Clu* has recently been shown to protect against age and aminoglycoside-induced hair cell loss, but without alteration of cochlear morphogenesis[35]. On the other hand, *Fst* has been previously proposed to play a central role during Shh-mediated cochlear morphogenesis and tonotopy[5]. Follistatin encodes an antagonist for TGFb/BMP signaling and is expressed in an apical to basal gradient in the cochlea[5,36]. It has been proposed that this gradient is required to generate a basal to apical gradient of ActivinA, a member of the TGFbeta superfamily. Moreover, this counter gradient of Activin A and Follistatin has recently been shown to instruct the timing of hair cell differentiation in the murine cochlea[36]. As mentioned above, early Shh signaling is crucial for establishing regional identity in the developing cochlea, including setting up the distinct apical pattern of *Fst* expression[5]. Recent work showed that *Fst* is required for the maintenance of apical cochlear identity as indicated by the loss of *Msx1* expression, *Fst* is dispensable for cochlear induction[37] (Table 2). In contrast to the apparent apical truncation of *Fst* mutants, cochlear outgrowth is more severely affected in *Meis2*$^{flox/flox}$; *Pax2*^{Cre} mutants, which exhibit a more severe disruption of cochlear outgrowth includes a loss of *Fst* and *Msx1* expression (Table 2). Therefore, the dysregulation of additional Shh responsive genes and/or other Meis2-

regulated genes are likely to contribute to the severe cochlear truncation observed in *Shh*$^{flox/-}$; *Foxg1*^{Cre} and *Meis2*$^{flox/flox}$; *Pax2*^{Cre} mutants, respectively. Further analysis of these genes will shed light into the specification of regional identity, proper outgrowth and coiling of the mammalian cochlea.

Acknowledgments

We would like to thank Irene Delgado and Miguel Torres for providing Meis mouse mutants and experimental advice and help. This work was supported by MinEco (BFU2016-76580-P) and Programa Estratégico Instituto de Biomedicina y Genética Molecular (IBGM), Escalera de Excelencia, Junta de Castilla y León (Ref. CLU-2019-02) and Programa Estratégico Instituto de Biomedicina y Genética Molecular (IBGM), Junta de Castilla y León (Ref. CCVC8485) to T.S. and by the National Research Foundation of Korea (NRF-2022R1A2C3007281, RS-2024-00400118) to J.B..

Experimental procedures

Transgenic mice

Mice carrying a floxed *Meis2* allele and a *Pax2*-Cre transgene have been described previously[17]. Experiments conformed to the institutional and national regulatory standards concerning animal welfare.

Screening for differentially regulated genes in *Meis2*$^{flox/flox}$; *Pax2*$^{Cre/+}$ mutants

RNA was isolated from E11,5 otic vesicles of wild type and *Meis2*$^{flox/flox}$; *Pax2*$^{Cre/+}$ mutants using the RNeasy Mini Kit (Qiagen) according to the manufacturer's instructions. Sequencing libraries were prepared using the NEBNext Ultra RNA Library Prep Kit for Illumina according to the manufacturer's instructions. Libraries were subjected to 2x75 bp paired-end sequencing on an Illumina NextSeq sequencer following the manufacturer´s protocol. Mapping of the reads to the GRCm38 reference genome was performed with Star software. Generation of count tables and differential expression was done by parsing Star

output with edgeR. Differentially expressed genes with an adjusted p value (false discovery rate) below 0.05 are listed in Table 1. The RNAseq data from this screen have been deposited at GEO with accession number GSE154787.

Quantitative reverse transcription polymerase chain reaction (qPCR)

Isolation of total RNA from otic vesicles was performed using TRIzol® Reagent (Invitrogen), following the manufacturer's protocol. RNA samples were quantified on a Spectrophotometer ND-1000 (NanoDrop, Thermo Fisher Scientific). Total RNA was used to synthesize cDNA with the High Capacity cDNA Reverse Transcription Kit (Applied Biosystems, Life Technologies). cDNA samples were amplified on a LightCycler® 480 II (Roche Molecular Diagnostics, Pleasanton, CA, USA) using SYBR® Green PCR Master Mix (Life Technologies). The thermocycling conditions consisted of an initial denaturation step of 10 minutes at 95°C, followed by 40 cycles at 95°C for 15 seconds and 60°C for 1 min. Primers for each of the genes studied in this work were: *Cyp26c1*, GGAGAAACAGACAGCAGAGC and GAAGAGGAGCTCTACAGCC; *Fst*, ACTAGAAGTACAGTACCAGGG and ATCCACCACACAAGTGGAGC; *Frem2, TGACCATCCTCACAGACAGG and TGGAAGGCTTAGAGAGGTCG; Clu, GAGCTCTGGTTTAGAAACTCC and TGCAAGCCCTGCCTGAAGC; Ptch1 AGACCAACATCACACGGACC and ATTCAGGACACATATGTGAGC*. Data were analysed using the Software version LCS480 1.5.0.39. Relative levels of mRNA expression were calculated according to the $2^{-\Delta\Delta Ct}$ method.

Immunofluorescence staining

Immunofluorescence staining was performed as previously described[5]. Primary antibodies used were anti-ARL13B (1:3000, generated from rabbit) and anti-MYO7A (1:200; Proteus biosciences, 256790). Secondary antibodies used were Alexa Fluor 488 antibodies (1:200, Thermo Fisher Scientific) and Alexa Fluor 568 Phalloidin (1:100, Thermo Fisher Scientific, A12380). Immunolabeled cochlear tissues were mounted with ProLong Gold Anti-fade Mountant (Thermo Fisher Scientific, P36930).

In situ hybridization

Inner ears dissected from E14.5 embryos were fixed in 4% paraformaldehyde overnight and embedded in Tissue-Tek optimum cutting temperature (OCT) compound. Inner ear tissues were sectioned at a 12 μm thickness using a cryostat (Thermo Fisher Scientific). Serial cochlear sections were collected from the base to the apex on to Superfrost Plus microscope slides (Thermo Fisher Scientific) and subjected to in situ hybridization as previously described[5]. Antisense RNA probes for *Ptch1, Gli1, Msx1, Fst, A2m*, and *Inhba* were prepared as previously described[5]. Images of in situ hybridization were acquired using a Leica DM2700 optical microscope.

References

1. Driver EC, Kelley MW. Development of the cochlea. *Development*. Jun 22 2020;147(12). https://doi.org10.1242/dev.162263.
2. Pyott SJ, Pavlinkova G, Yamoah EN, Fritzsch B. Harmony in the Molecular Orchestra of Hearing: Developmental Mechanisms from the Ear to the Brain. *Annu Rev Neurosci*. Feb 15 2024. https://doi.org10.1146/annurev-neuro-081423-093942.
3. Brown AS, Epstein DJ. Otic ablation of smoothened reveals direct and indirect requirements for Hedgehog signaling in inner ear development. *Development*. Sep 2011;138(18):3967-76. https://doi.org10.1242/dev.066126.
4. Riccomagno MM, Martinu L, Mulheisen M, Wu DK, Epstein DJ. Specification of the mammalian cochlea is dependent on Sonic hedgehog. *Genes Dev*. Sep 15 2002;16(18):2365-78. https://doi.org10.1101/gad.1013302.
5. Son EJ, Ma JH, Ankamreddy H, et al. Conserved role of Sonic Hedgehog in tonotopic organization of the avian basilar papilla and mammalian cochlea. *Proc Natl Acad Sci U S A*. Mar 24 2015;112(12):3746-51. https://doi.org10.1073/pnas.1417856112.
6. Bok J, Zenczak C, Hwang CH, Wu DK. Auditory ganglion source of Sonic hedgehog regulates timing of cell cycle exit and differentiation of mammalian cochlear hair cells. *Proc Natl Acad Sci U S A*. Aug 20 2013;110(34):13869-74. https://doi.org10.1073/pnas.1222341110.
7. Muthu V, Rohacek AM, Yao Y, et al. Genomic architecture of Shh-dependent cochlear morphogenesis. *Development*. Sep 19 2019;146(18). https://doi.org10.1242/dev.181339.
8. Bouchard M, de Caprona D, Busslinger M, Xu P, Fritzsch B. Pax2 and Pax8 cooperate in mouse inner ear morphogenesis and innervation. *BMC Dev Biol*. Aug 20 2010;10:89. https://doi.org10.1186/1471-213X-10-89.
9. Chizhikov VV, Iskusnykh IY, Fattakhov N, Fritzsch B. Lmx1a and Lmx1b are Redundantly Required for the Development of Multiple Components of the Mammalian Auditory System. *Neuroscience*. Jan 1 2021;452:247-264. https://doi.org10.1016/j.neuroscience.2020.11.013.
10. Filova I, Bohuslavova R, Tavakoli M, Yamoah EN, Fritzsch B, Pavlinkova G. Early Deletion of Neurod1 Alters Neuronal Lineage Potential and Diminishes Neurogenesis in the Inner Ear. *Front Cell Dev Biol*. 2022;10:845461. https://doi.org10.3389/fcell.2022.845461.
11. Filova I, Pysanenko K, Tavakoli M, et al. ISL1 is necessary for auditory neuron development and contributes toward tonotopic organization. *Proc Natl Acad Sci U S A*. Sep 13 2022;119(37):e2207433119. https://doi.org10.1073/pnas.2207433119.
12. Kopecky B, Santi P, Johnson S, Schmitz H, Fritzsch B. Conditional deletion of N-Myc disrupts neurosensory and non-sensory development of the ear. *Dev Dyn*. Jun 2011;240(6):1373-90. https://doi.org10.1002/dvdy.22620.
13. Ma Q, Anderson DJ, Fritzsch B. Neurogenin 1 null mutant ears develop fewer, morphologically normal hair cells in smaller sensory epithelia devoid of innervation. *J Assoc Res Otolaryngol*. Sep 2000;1(2):129-43. https://doi.org10.1007/s101620010017.
14. Song H, Morrow BE. Tbx2 and Tbx3 regulate cell fate progression of the otic vesicle for inner ear development. *Dev Biol*. Feb 2023;494:71-84. https://doi.org10.1016/j.ydbio.2022.12.003.
15. Xu J, Li J, Zhang T, et al. Chromatin remodelers and lineage-specific factors interact to target enhancers to establish proneurosensory fate within otic ectoderm. *Proc Natl Acad Sci U S A*. Mar 23 2021;118(12). https://doi.org10.1073/pnas.2025196118.
16. Schulte D, Geerts D. MEIS transcription factors in development and disease. *Development*. Aug 15 2019;146(16). https://doi.org10.1242/dev.174706.

17. Duran Alonso MB, Vendrell V, Lopez-Hernandez I, et al. Meis2 Is Required for Inner Ear Formation and Proper Morphogenesis of the Cochlea. *Front Cell Dev Biol*. 2021;9:679325. https://doi.org10.3389/fcell.2021.679325.
18. Duncan JS, Fritzsch B. Continued expression of GATA3 is necessary for cochlear neurosensory development. *PLoS One*. 2013;8(4):e62046. https://doi.org10.1371/journal.pone.0062046.
19. Matei V, Pauley S, Kaing S, et al. Smaller inner ear sensory epithelia in Neurog 1 null mice are related to earlier hair cell cycle exit. *Dev Dyn*. Nov 2005;234(3):633-50. https://doi.org10.1002/dvdy.20551.
20. Pauley S, Lai E, Fritzsch B. Foxg1 is required for morphogenesis and histogenesis of the mammalian inner ear. *Dev Dyn*. Sep 2006;235(9):2470-82. https://doi.org10.1002/dvdy.20839.
21. Gao J, Skidmore JM, Cimerman J, et al. CHD7 and SOX2 act in a common gene regulatory network during mammalian semicircular canal and cochlear development. *Proc Natl Acad Sci U S A*. Mar 5 2024;121(10):e2311720121. https://doi.org10.1073/pnas.2311720121.
22. de Lope C, Garcia-Lucena R, Magarinos M, et al. Dysfunction of programmed embryo senescence is linked to genetic developmental defects. *Development*. May 1 2023;150(9). https://doi.org10.1242/dev.200903.
23. Yao H, Hill SF, Skidmore JM, et al. CHD7 represses the retinoic acid synthesis enzyme ALDH1A3 during inner ear development. *JCI Insight*. Feb 22 2018;3(4). https://doi.org10.1172/jci.insight.97440.
24. Urness LD, Wang X, Doan H, et al. Spatial and temporal inhibition of FGFR2b ligands reveals continuous requirements and novel targets in mouse inner ear morphogenesis. *Development*. Dec 18 2018;145(24). https://doi.org10.1242/dev.170142.
25. Galvez H, Tena JJ, Giraldez F, Abello G. The Repression of Atoh1 by Neurogenin1 during Inner Ear Development. *Front Mol Neurosci*. 2017;10:321. https://doi.org10.3389/fnmol.2017.00321.
26. Yu G, Wang LG, He QY. ChIPseeker: an R/Bioconductor package for ChIP peak annotation, comparison and visualization. *Bioinformatics*. Jul 15 2015;31(14):2382-3. https://doi.org10.1093/bioinformatics/btv145.
27. Buenrostro JD, Giresi PG, Zaba LC, Chang HY, Greenleaf WJ. Transposition of native chromatin for fast and sensitive epigenomic profiling of open chromatin, DNA-binding proteins and nucleosome position. *Nat Methods*. Dec 2013;10(12):1213-8. https://doi.org10.1038/nmeth.2688.
28. Vierstra J, Stamatoyannopoulos JA. Genomic footprinting. *Nat Methods*. Mar 2016;13(3):213-21. https://doi.org10.1038/nmeth.3768.
29. Bok J, Dolson DK, Hill P, Ruther U, Epstein DJ, Wu DK. Opposing gradients of Gli repressor and activators mediate Shh signaling along the dorsoventral axis of the inner ear. *Development*. May 2007;134(9):1713-22. https://doi.org10.1242/dev.000760.
30. Driver EC, Pryor SP, Hill P, et al. Hedgehog signaling regulates sensory cell formation and auditory function in mice and humans. *J Neurosci*. Jul 16 2008;28(29):7350-8. https://doi.org10.1523/JNEUROSCI.0312-08.2008.
31. Moon KH, Ma JH, Min H, et al. Dysregulation of sonic hedgehog signaling causes hearing loss in ciliopathy mouse models. *Elife*. Dec 31 2020;9. https://doi.org10.7554/eLife.56551.
32. Albano RM, Arkell R, Beddington RS, Smith JC. Expression of inhibin subunits and follistatin during postimplantation mouse development: decidual expression of activin and expression of follistatin in primitive streak, somites and hindbrain. *Development*. Apr 1994;120(4):803-13. https://doi.org10.1242/dev.120.4.803.

33. Urness LD, Paxton CN, Wang X, Schoenwolf GC, Mansour SL. FGF signaling regulates otic placode induction and refinement by controlling both ectodermal target genes and hindbrain Wnt8a. *Dev Biol*. Apr 15 2010;340(2):595-604. https://doi.org10.1016/j.ydbio.2010.02.016.
34. Uehara M, Yashiro K, Mamiya S, et al. CYP26A1 and CYP26C1 cooperatively regulate anterior-posterior patterning of the developing brain and the production of migratory cranial neural crest cells in the mouse. *Dev Biol*. Feb 15 2007;302(2):399-411. https://doi.org10.1016/j.ydbio.2006.09.045.
35. Zhao X, Henderson HJ, Wang T, Liu B, Li Y. Deletion of Clusterin Protects Cochlear Hair Cells against Hair Cell Aging and Ototoxicity. *Neural Plast*. 2021;2021:9979157. https://doi.org10.1155/2021/9979157.
36. Prajapati-DiNubila M, Benito-Gonzalez A, Golden EJ, Zhang S, Doetzlhofer A. A counter gradient of Activin A and follistatin instructs the timing of hair cell differentiation in the murine cochlea. *Elife*. Jun 12 2019;8. https://doi.org10.7554/eLife.47613.
37. Koo HY, Kim MA, Min H, et al. Follistatin regulates the specification of the apical cochlea responsible for low-frequency hearing in mammals. *Proc Natl Acad Sci U S A*. Jan 3 2023;120(1):e2213099120. https://doi.org10.1073/pnas.2213099120.
38. Tateya T, Imayoshi I, Tateya I, et al. Hedgehog signaling regulates prosensory cell properties during the basal-to-apical wave of hair cell differentiation in the mammalian cochlea. *Development*. Sep 2013;140(18):3848-57. https://doi.org10.1242/dev.095398.

Figure 1

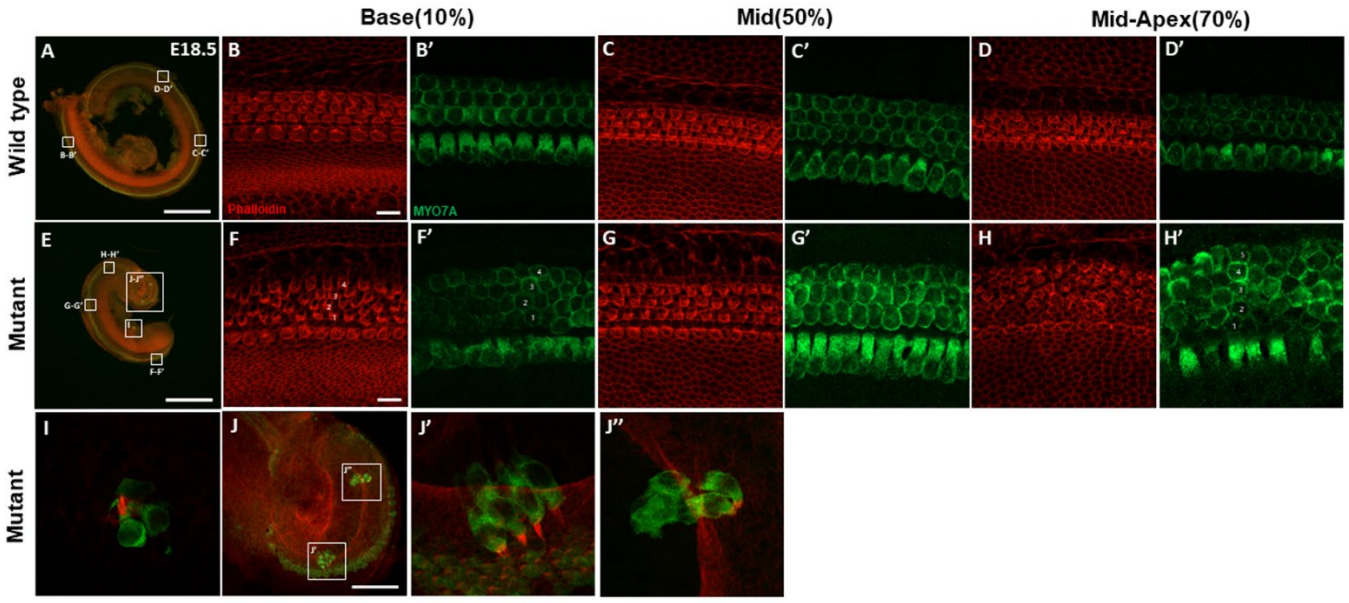

Figure 1. *Meis2*$^{flox/flox}$; *Pax2*$^{Cre/+}$ cochlea shows defective cochlear outgrowth and organ of Corti patterning.

E18.5 wild type and *Meis2*$^{flox/flox}$; *Pax2*$^{Cre/+}$ cochleas were stained with phalloidin to visualize hair bundles (red) and anti-Myo7a antibody to visualize hair cells (green). (A-D') In E18.5 wild type cochlea, one row of inner hair cell (IHC) and three rows of outer hair cells (OHCs) were observed. (E-J'') In *Meis2*$^{flox/flox}$; *Pax2*$^{Cre/+}$ cochlea, the cochlear length was severely shortened compared to wild type (E) and four rows (F,F') or five rows of OHC (H,H') were often observed. Vestibular-like hair cells were observed in the greater epithelial ridge region of the apical cochlea (I-J''). Scale bar in (A, E) is 500um; scale bar in (B-D', F-H', I, J'-J'') is 10um.

Figure 2

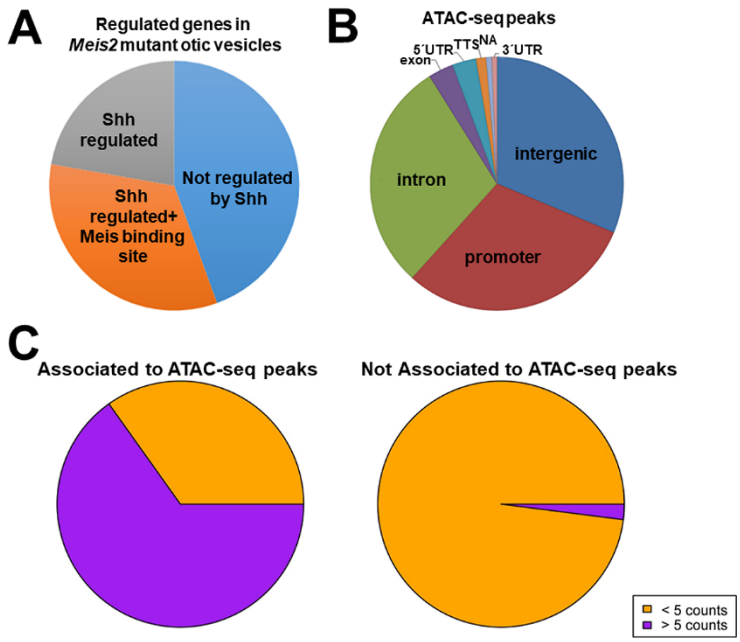

Figure 2. Distribution of Shh-regulated genes in *Meis2* mutant otic vesicles and association of open chromatin with otic gene expression.

Pie chart showing the relative distribution of genes differentially expressed in *Meis2* mutant otic vesicles and regulation of these genes by Meis2 (A). Pie chart showing the distribution of open chromatin detected by ATAC-sequencing in mouse otic vesicles (B). Pie charts showing the distribution of otic genes with a relatively high (purple) or low (orange) level of expression within open chromatin detected by ATAC-sequencing (C). Abbreviations: UTR: untranslated region; TTS: transcription termination site; NA: not associable

Figure 3

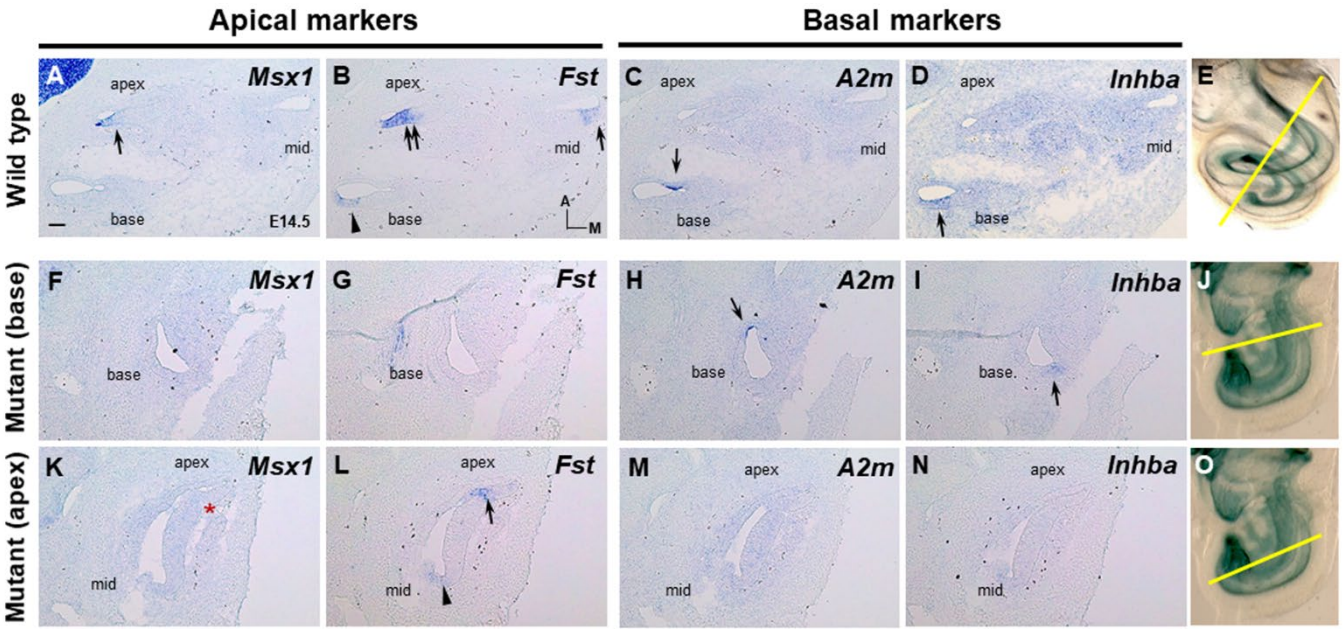

Figure 3. Conditional loss of *Meis2* in inner ear results in shortened cochlea and loss of cochlear identity at the apex

(A-D) In E14.5 wild type cochlea, *A2m* and *Inhba* are expressed in basal cochlea (C-D, arrows) whereas *Fst* and *Msx1* are expressed strongly in apical cochlea (A-B, arrows). (F-N) In E14.5 *Meis2*$^{flox/flox}$; *Pax2*$^{Cre/+}$ cochlea, the basal markers are expressed in the basal turn (H-I, arrows), whereas the apical markers are either lost (*Msx1* in K, asterisk) or weakly expressed (*Fst* in L, arrow) in middle and apical turns (K-N). The different planes of sections are indicated on the right (E, J, O, modified from Duran Alonso et al., 2021). Scale bar in A (100 um) applies to all section panels.

1
2
3

Table 1

Gene	MGI	Expression in otic vesicle/cochlea	Fold-regulation	Shh mutant	open chromatin/Meis site
Cyp26c1	2679699	ventral otic vesicle	0.6x	down	+/+
Fst	95586	ventral otic vesicle/sensory tissue	0.3x	down	+
Frem2	2444465	non-sensory tissue	0.6x	down	+/+
Clu	12759	ventral otic vesicle/sensory tissue	0.3x	down	+
Lars2	2142973	n.d.	0.6x	n.l.	+
Acta2	87909	n.d.	0.3x	n.l.	-
Alcam	1313266	cochlear ganglion	1.6x	up	+/+
Aldh1a2	5819521	medial-lateral otic vesicle/ non-sensory tissue	0.3x	n.l.	+/+
Bcam	1929940	n.d.	0.6x	down	+/+
Lin28a	1890546	ventral and dorsal otic vesicle	0.4x	n.l.	+/+
Cacna1g	1201678	n.d.	1.6x	up	+
Tgfb2	98726	otic vesicle/sensory epithelium	1.6x	n.l.	+
Irs4	1338009	n.d.	0.4x	n.l.	+
Col12a1	88448	otic capsule	1.7x	up	+

Table 1: Genes differentially regulated in *Meis2*$^{flox/flox}$; *Pax2*^{Cre} mouse mutants. The reference number of the genes at Mouse Genome Informatics (MGI), their expression in the otic vesicle and/or cochlea, their fold-regulation listed according to significance (p-value), their regulation in Shh mutants[7], the presence of open chromatin and a Meis binding site are indicated. Abbreviations: n.d.: not determined; n.l.: not listed

Table 2

Mouse mutant	*Fst* (E11)	*Fst* (E15)	*Msx1* (E15)	Cochlea
Meis2$^{flox/flox}$; *Pax2*^{Cre}	reduced	reduced	absent	severe truncation
Fst$^{-/-}$ [37]	absent	absent	absent (present at E11)	apical truncation
Shh$^{flox/-}$; *Foxg1*^{Cre} [5,37]	n.d.	present	present	severe truncation
Smo$^{flox/flox}$; *Emx2*^{Cre} [37,38]	present	present	reduced	apical truncation
Smo$^{flox/-}$; *Foxg1*^{Cre} [3,7]	reduced	n.a.	n.a.	loss of cochlea

Table 2: Expression of *Fst* and *Msx1* at the indicated embryonic stages (E) and effects on cochlear outgrowth in the indicated mouse mutants. Abbreviations: n.d.: not determined, n.a.: not applicable

Supplementary Figure 1

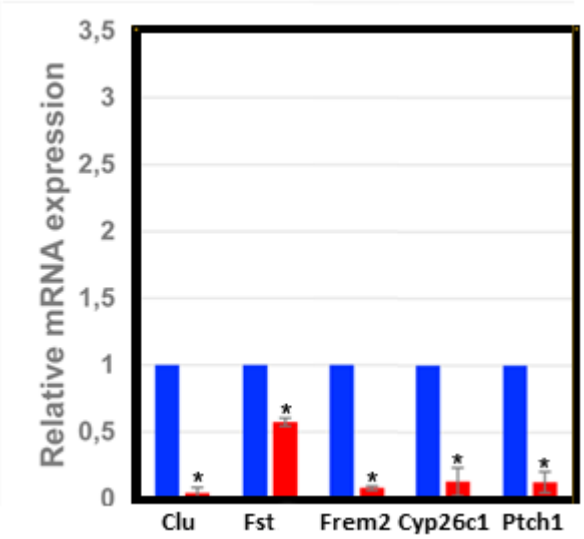

Significantly reduced mRNA expression of the indicated genes was observed in E11,5 otic vesicles isolated from *Meis2*$^{flox/flox}$; *Pax2*$^{Cre/+}$ mutants (red bars) in comparison to wild-type otic vesicles (blue bars). Asterisks: p-value<0,05.

Supplementary Figure 2

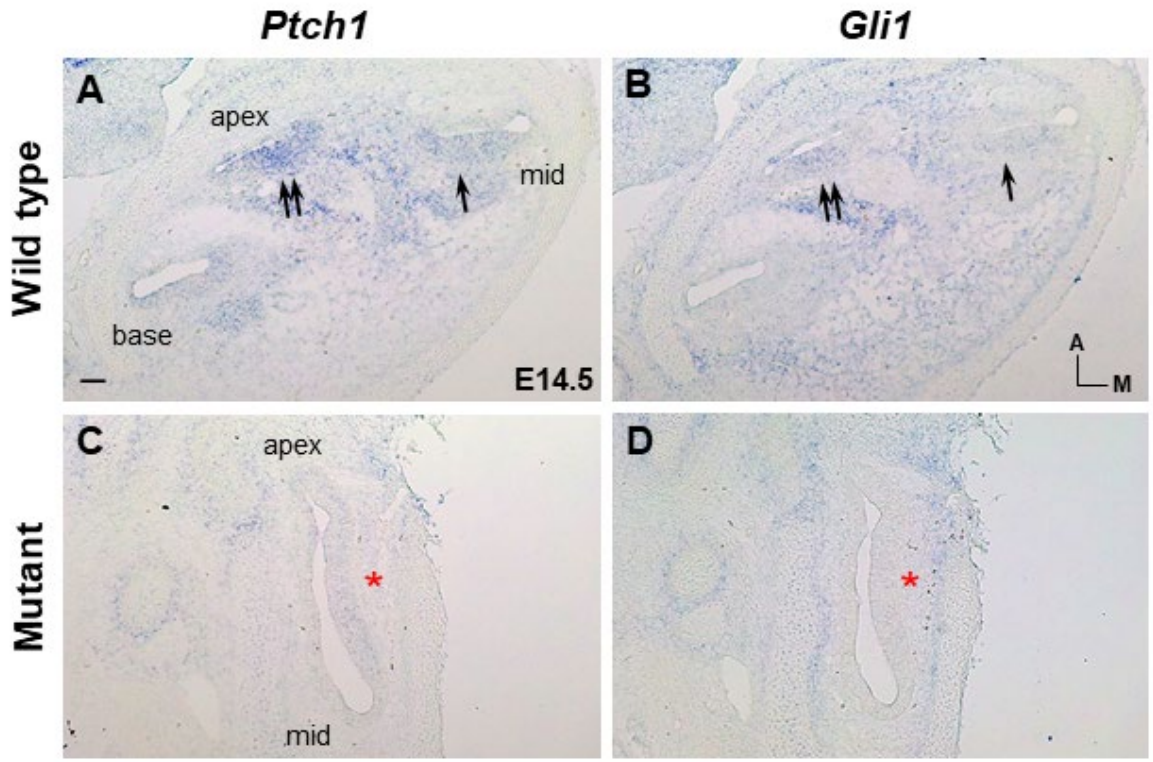

In E14.5 wild-type cochlea, Shh target genes *Ptch1* and *Gli1* are detected in a graded pattern with stronger expression in the apex (A, B; arrows) and weaker towards the base. In *Meis2*$^{flox/flox}$; *Pax2*$^{Cre/+}$ mutants, *Ptch1* and *Gli1* expression are strongly reduced in the cochlea (C, D, asterisks).